IEEE Photonics Journal
An IEEE Photonics Society Publication

Open Access

Enhanced Spurious-Free Dynamic Range in Intensity-Modulated Analog Photonic Link Using Digital Postprocessing

Volume 6, Number 2, April 2014

Yan Cui
Yitang Dai
Feifei Yin
Qiang Lv
Jianqiang Li
Kun Xu
Jintong Lin

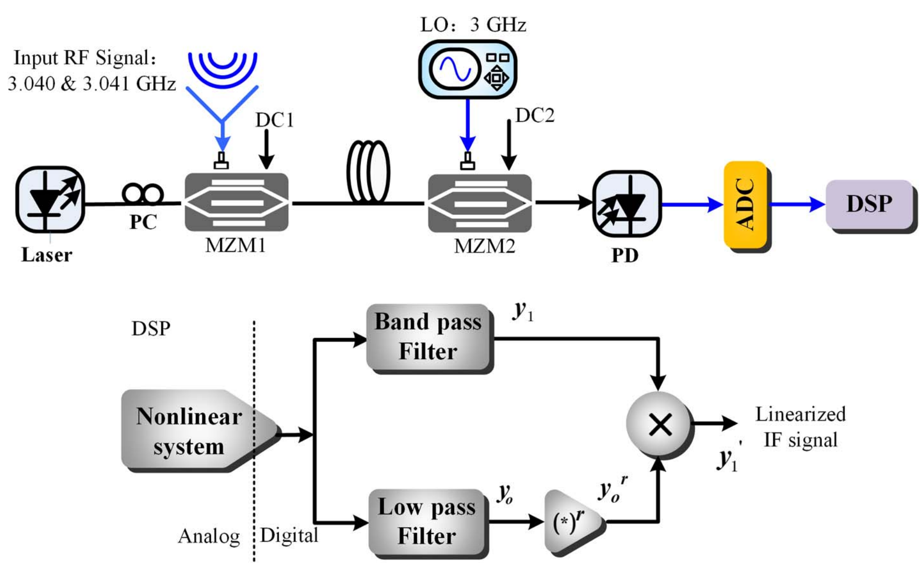

DOI: 10.1109/JPHOT.2014.2308196
1943-0655 © 2014 IEEE

Enhanced Spurious-Free Dynamic Range in Intensity-Modulated Analog Photonic Link Using Digital Postprocessing

Yan Cui,[1] Yitang Dai,[1] Feifei Yin,[1] Qiang Lv,[2,3] Jianqiang Li,[1] Kun Xu,[1] and Jintong Lin[1]

[1]State Key Laboratory of Information Photonics and Optical Communications, Beijing University of Posts and Telecommunications, Beijing 100876, China
[2]The 54th Research Institute of CETC, Shijiazhuang 050081, China
[3]Science and Technology on Information Transmission and Dissemination in Communication Networks Laboratory, Shijiazhuang 050081, China

DOI: 10.1109/JPHOT.2014.2308196

Manuscript received January 20, 2014; revised February 16, 2014; accepted February 20, 2014. Date of publication February 25, 2014; date of current version March 5, 2014. This work was supported in part by the 973 Program under Grant 2012CB315705; by the NSFC Program under Grants 61271042, 61107058, 61302016, and 61335002, and by NCET-13-0682. Corresponding author: Y. Cui (e-mail: cuiyan1128@bupt.edu.cn).

Abstract: In this paper, a post digital linearization technique is proposed and demonstrated for a conventional intensity-modulation direct-detection analog photonic link. Instead of precisely emulating the transfer function of the whole nonlinear system in the digital domain, the key distortion information is directly acquired from hardware. By low biasing the Mach–Zehnder modulator, linearization can be achieved through simply multiplying the distorted signal by the coreceived low-pass band. Theory analysis shows that only the bias angle should be known by the algorithm, whereas the simulation shows adequate tolerance. The low bias angle also results in an improved link gain. The experiment shows a well-suppressed third-order intermodulation distortion (IMD3). With the optical down conversion, we demonstrate a spurious-free dynamic range increasing from 103.2 to 123.3 dB in a 1-Hz bandwidth.

Index Terms: Radio frequency photonics, fiber optics systems, digital signal processing.

1. Introduction

Analog photonic link has become very attractive during the past years for both commercial and military applications, such as antenna remoting, radio astronomy, etc. [1], [2]. In some challenging applications such as military use, analog photonic link must meet the stringent performance requirements in terms of dynamic range, gain, and other figures of merit. The spurious-free dynamic range (SFDR) is one of the most important parameters. External intensity modulation by MZM is adopted in most links due to its simple structure, capacity for high speed, stability, and commercial availability. But the intrinsical nonlinear transfer function of MZM may introduce both harmonic crosstalk and intermodulation distortion, which will deteriorate the link's dynamic range, unfortunately. In most applications where only sub-octave span is used, the third-order intermodulation distortion (IMD3) components should be particularly considered as they lie very close to the radio frequency (RF) carriers and are impossible to be eliminated by simple RF filtering. The IMD3 will then significantly reduce the SFDR performance of the link [3].

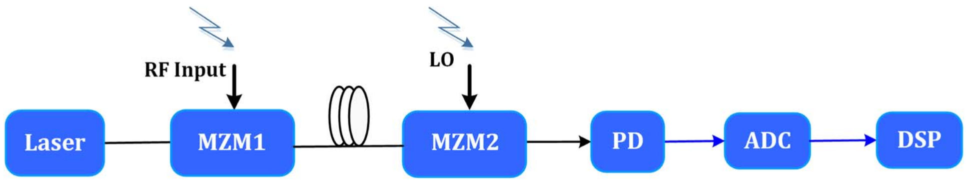

Fig. 1. General IMDD analog photonic link with optical down-conversion and DSP-based linearization. LO: local oscillator; ADC: analog-to-digital converter.

Previously, a variety of techniques have been investigated to improve the linearization of the MZM-based intensity modulated analog photonic link. The basic design idea behind most of the strategies is to generate a well-designed and matched distortion that can be used to cancel out exactly the existing one. Extend linearity is then achieved by using electronic pre-distortion [4], which however shows limitation on the capacity for higher RF carrier frequency and larger bandwidth. The same limitation shows in the feed-forward approach [5], where the matched IMD3 is generated by a mixed electronic-optical way. The matched distortion has been also generated in many all-optical schemes in order to obtain a high carrier frequency ability. In these schemes, an additional "nonlinear" link is carefully designed, and both distortions cancel each other at the photo detector (PD). Dual MZM in parallel [6] or series [7] are usually required, and strict RF signal and optical power split ratio for both links, as well as time delay between them, are demanded, which increases the system complexity. Besides, either signal or optical power split results in the additional loss of the analog photonic link. Linearized analog photonic link with phase modulation and direct detection is especially attractive and proposed in [8], [9], which can get rid of DC bias control requirement and achieve certain improvement in the SFDR. Other linearization approaches based on phase modulator and optical-phase-locked-loop [10], dual parallel MZM [11] and dual-electrode modulator [12] are also proposed but with additional complexity, unfortunately.

Recently the digital post distortion suppression by digital signal processing (DSP) has been demonstrated and especially attractive due to its flexibility and superior linearization ability. The optical down-conversion combined with DSP has been considered as a promising strategy for remote RF receiving. Digital linearization for phase and polarization modulation has been widely discussed, for its linear modulation and demodulation at both ends [13]–[15]. In experiment, dynamic range as high as 124 dB @ 1 Hz bandwidth has been demonstrated [15]. With optical down-conversion, SFDR of 120 dB is reported in [16]. Note that such performance costs a complicated in-phase/quadrature (I/Q) demodulation scheme. On the contrary, the digital linearization for intensity modulated photonic link shows a much simpler hardware. Fig. 1 shows a typical intensity-modulation direct-detection (IMDD) link where the optical down-conversion and digital post linearization are included.

Without complicating the traditional design, an effective digital linearization algorithm for intensity modulation will be widely used in the receive end of future radio-over-fiber applications. However, few experiments have been demonstrated, since the intensity-modulated link has a more complex transfer function than the phase or polarization modulated one with I/Q demodulation. Though it is well-known that the MZM has a sinusoidal transfer function, its nonlinear dependence on the optical power, the responsivity of the photodiode (PD), the bias angle and half-wave voltage of the MZM, etc. making it actually impossible to reconstruct the RF signal by a direct inverse of the transfer function. In [17] the linearization algorithm depends on the precise PD responsivity and the input optical power. In [18], authors demonstrate a brilliant algorithm where an equalization filter and a transfer function emulator are used instead of the direct inverse. In [19], such algorithm is iterated so that the SFDR of 120 dB @ 1 Hz is achieved without down-conversion. However, multiple link parameters related to the equalizer and emulator have still to be precisely determined to match the physical system, which may otherwise result in significant imperfections.

Besides, the down-conversion is all excluded where the analog to digital converter (ADC) may show difficulty for RF signal with high carrier frequency [17]–[19].

In order to release the above requirement, we propose and demonstrate a novel DSP algorithm for digital linearization of MZM-based intensity-modulated analog photonic link in this paper. In our approach, the MZM is low-biased, and the nonlinear distortion information is acquired with hardware, i.e., the digital low-pass band after PD, instead of building a digital transfer function emulator. By precisely fixing the bias angle of MZM only, the IMD3 can be suppressed exactly. The algorithm is compatible with optical down-conversion. Experimentally, we demonstrate an SFDR improvement from 103.2 dB to 123.3 dB @ 1 Hz bandwidth in a down-conversion link. An obvious increase of the link gain is also demonstrated due to the use of the low-biased design.

2. Operation Principle of the Scheme

Fig. 1 shows the schematic diagram of the proposed digitally linearized MZM-based IMDD link. The output of the optical source is modulated by an electrical band-pass signal

$$x(t) = A(t)\cos(\omega_{\mathrm{RF}} t). \tag{1}$$

Its bandwidth is less than an octave span and the RF angle frequency is ω_{RF}. The MZM1 is low biased. As a result, such link contains all orders of harmonics. In general, we assume that the link voltage-to-voltage transfer function is

$$y = a_0 + a_1 x + a_2 x^2 + a_3 x^3. \tag{2}$$

Note that higher order harmonics than three are ignored since their minor contributions. At the receive end, only the low-pass band, y_o, and the fundamental band around ω_{RF}, y_1, are considered. Substitute (1) into (2) and we can get the corresponding expressions as

$$\begin{aligned} y_0(t) &= a_0 + \frac{a_2}{2} A(t)^2; \\ y_1(t) &= \left[a_1 + \frac{3a_3}{4} A(t)^2 \right] \cdot A(t)\cos(\omega_{\mathrm{RF}} t). \end{aligned} \tag{3}$$

We can clearly observe the IMD3 inside y_1 due to the additional modulation by $A(t)^2$. Also, we can observe that such modulation is contained in y_o. So we propose that the distortion can be eliminated by the following algorithm:

$$\begin{aligned} y_1' = y_0^{\gamma} y_1 &\approx a_0^{\gamma} a_1 \left(1 + \frac{\gamma a_2}{2a_0} A^2 + \frac{3a_3}{4a_1} A^2 \right) \cdot A\cos\omega t \\ &= a_0^{\gamma} a_1 A\cos\omega t. \end{aligned} \tag{4}$$

Equation (4) shows that the nonlinearity compensation occurs when

$$\gamma = -\frac{3}{2} \frac{a_0}{a_2} \frac{a_3}{a_1}. \tag{5}$$

Such condition can be applied to any specific link such as the MZM-based IMDD one, where the voltage-to-voltage transfer function is

$$y = \frac{R_{\mathrm{PD}} I_{\mathrm{PD}} Z_{\mathrm{PD}}}{1 + \sin\varphi} \left[1 - \sin\left(\frac{\pi}{V_{\pi,\mathrm{RF}}} x - \varphi \right) \right] \tag{6}$$

where $V_{\pi,\mathrm{RF}}$ and φ are the RF half-wave voltage and the bias angle that shifted away from the quadrature point, respectively, of MZM1, I_{PD} is the average optical power received by the PD, and R_{PD} and Z_{PD} are the RF responsivity and equivalent output impedance of the PD, respectively. By approximately expanding (6), one can easily calculate all the four coefficients $(a_0 \sim a_3)$ defined by (2), and can get

$$\begin{aligned} a_0 &= R_{\mathrm{PD}} I_{\mathrm{PD}} Z_{\mathrm{PD}} \\ a_1 &= -\frac{\cos\varphi}{1+\sin\varphi} R_{\mathrm{PD}} I_{\mathrm{PD}} Z_{\mathrm{PD}} \frac{\pi}{V_{\pi,\mathrm{RF}}} \\ a_2 &= -\frac{1}{2}\frac{\sin\varphi}{1+\sin\varphi} R_{\mathrm{PD}} I_{\mathrm{PD}} Z_{\mathrm{PD}} \left(\frac{\pi}{V_{\pi,\mathrm{RF}}}\right)^2 \\ a_3 &= \frac{1}{6}\frac{\cos\varphi}{1+\sin\varphi} R_{\mathrm{PD}} I_{\mathrm{PD}} Z_{\mathrm{PD}} \left(\frac{\pi}{V_{\pi,\mathrm{RF}}}\right)^3. \end{aligned} \tag{7}$$

Substitute (7) into (5), and we finally get

$$\gamma = -\frac{1+\sin\varphi}{2\sin\varphi}. \tag{8}$$

With a second MZM cascaded in series, the RF frequency down-conversion is accomplished in the optical domain. Due to the nonlinearity of the second MZM, both difference-frequency (the desired intermediate frequency) and sum-frequency of the RF signal and the local oscillator are generated. The sum-frequency component is not a problem. This is due to the fact that the sum-frequency component is beyond the operational bandwidth of system. After optical down-conversion, y_o is still there while y_1 is moved to intermediate frequency (IF). Though y_1 and y_o get additional loss, the ratios of a_0/a_2 and a_3/a_1 are kept unchanged. As a result, the distortion information acquisition and the post-compensation algorithm shown in (5) and (8) work with and without optical down-conversion. The only influence brought by the cascaded MZM is the gain penalty, unfortunately.

Our proposal is different from the previous ones where the whole link transfer function has to be precisely emulated in digital domain. Actually, the key distortion information, y_o, is generated with the signal, y_1, after MZM1 and is acquired with hardware at the receive end, which simplifies our algorithm and release the demand of link parameter estimations: only the bias angle of MZM1 should be precisely known by the algorithm, which can be easily achieved now by commercial available bias control circuit [20]. Such property shows a robust signal reconstruction independent from other link parameters such as optical power, link loss, RF-frequency-related PD responsivity, etc.

In order to get an effective γ, the bias angle should be out of the quadrature point. In our design low bias is selected, i.e., $\sin\varphi < 0$. For conventional PDs the input power is limited to only a few dBm to get a linear response. The fiber delivery also shows an optical power limitation due to the stimulated Brillouin scattering. When the maximum input optical power of the PD is less than the maximum value the optical source can offer, (6) shows that the link gain can be further increased by a low bias angle as $\sin\varphi < 0$. The gain improvement is $\cos^2\varphi/(1+\sin\varphi)^2$ according to (6), compared with the quadrature bias. So our design combines the nonlinearity cancellation and gain increase, rather than other schemes where the linearization costs additional loss. For example, if MZM1 is biased so that $\sin\varphi = -1/3$, the link gain improvement is 3 dB, while $\gamma = 1$, i.e., the IMD3 can be easily removed through multiplying the down-converted IF directly by the co-received low-pass signal. Larger link gain can be achieved by further increase the optical source power while decreasing the bias angle. Note that MZM2, which is used for the down-conversion, should be at the quadrature bias to maximize the down-conversion efficiency.

3. Simulation and Experiment Results

Fig. 2(a) shows our experiment setup. The continuous-wave (CW) laser source operating at a wavelength of 1550 nm is used as the optical carrier. The principal axis of the output light beam is aligned with that of the following standard MZM1 (EOSpace, 20 GHz). Two RF tones, with frequencies of 3.040 GHz and 3.041 GHz, respectively, are generated by two vector signal

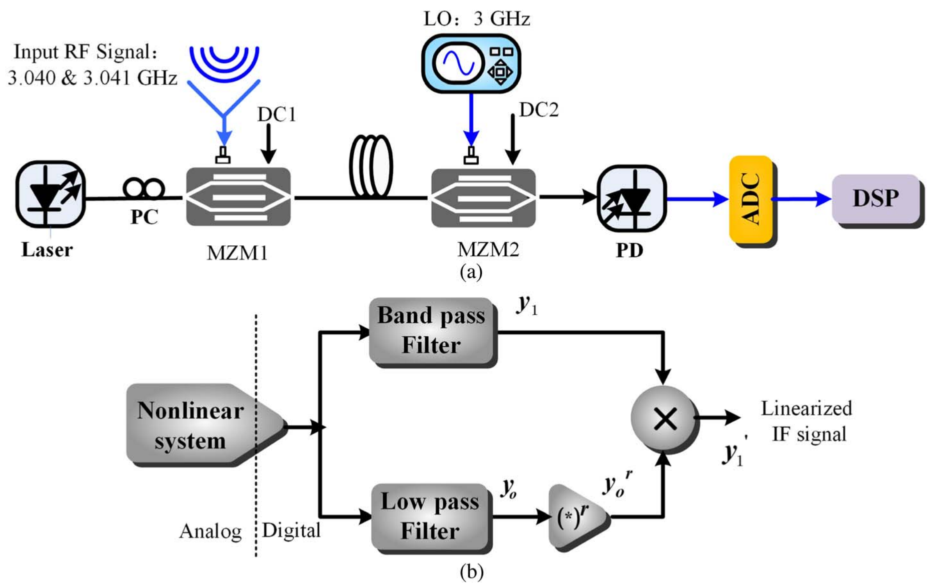

Fig. 2. (a) Experimental setup. (b) Block diagram of the proposed linearization algorithm.

generators (Agilent E8267D) and used to drive the modulator. The bias angle is fixed at $-43°$, corresponding to a gain increase of about 7.2 dB compared with a quadrature biased link under the same input power of the PD. After a short single mode fiber delivery, the optical signal is modulated again by MZM2 which is driven by a 3 GHz LO. The optical signal is received by a PD with responsivity of 0.92 A/W (EM4, 20 GHz). As a result, the RF signal is down-converted to IF band around 40 MHz. The output voltage is recorded by an ADC (ADLink with 14-bit level and 200 MS/s). Fig. 2(b) shows the following DSP algorithm. The digitalized voltage is firstly filtered by a low-pass filter and a band-pass filter, respectively, in order to get the distortion information, y_o, and the down-converted IF signal, y_1. The bandwidths of both filters are required to match the signal bandwidth. Then the γth power of y_o is calculated. y_o^γ times y_1 is the final output.

The above setup is simulated to verify the validity of the proposed distortion hardware acquisition and the corresponding algorithm. We assume Z_{PD} is 50 Ω, the half wave voltage of both MZMs is 3.5 V, I_{PD} is 3 dBm, where the parameters follow those in the experiment. Power of each input RF tone is 2 dBm. The bias angle, φ, is scanned from $-5°$ to $-60°$, and the down-converted signals are recorded. For each record under certain φ, the distortion suppression algorithm in Fig. 2(b) is performed under a scanned γ (from 0.1 to 5). For each case the power ratio between the fundamental frequency (40 MHz or 41 MHz) and the distortion part (39 MHz or 42 MHz) is calculated, while the contour plot is shown in Fig. 3.

Note that without digital linearization the power ratio is about 36 dB, which stands for every bias angle. After the linearization, the suppressed ratios are shown in the contour plot (the blank area corresponds to the states where the linearization fails, i.e., the ratio is less than 36 dB). One can clearly see a ridge where the distortion is suppressed greatly under an optimized γ, which is consistent well with the theoretical prediction by (8) (shown as the square line in Fig. 3). Besides, one can see the increased link gain as the bias angle decreases, while the tolerance of γ for an effective linearization is also decreased.

On the premise that the same optical power is launched, the link gain is reduced as the bias angle is shifted towards 180°. But the reduction of the slope efficiency can be compensated by increasing the input optical power [6]. Due to the limited maximum output optical power (16 dBm) of the laser source that we have, a $-43°$ bias angle is selected to make the best use of the available laser power, while a 3 dBm I_{PD} is maintained before the photodiode (PD). Note that higher link gain can be achieved by using the low bias technique, as compared with that of the quadrature biased case, when I_{PD} is the same for both cases. The gain advantage is easy to be observed in Fig. 3. It is also

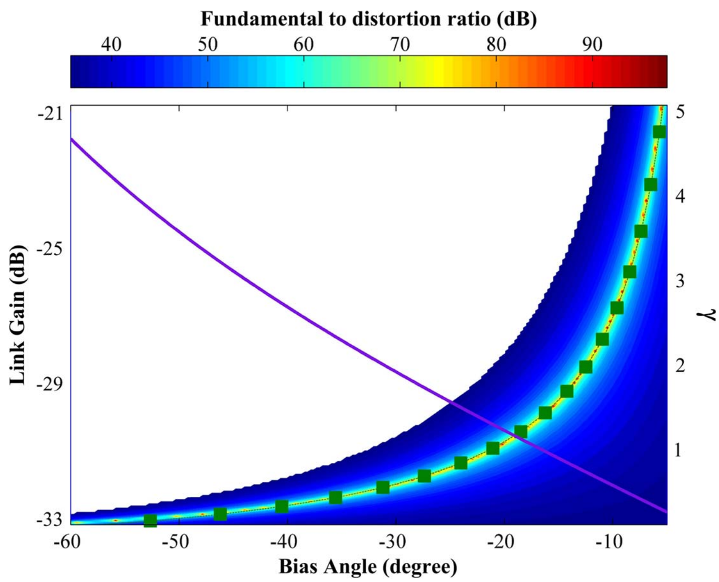

Fig. 3. Contour plot of the power ratio between the fundamental and distortion under different combination of bias angle and γ. Green square line: the theoretical prediction of γ by (8); Solid purple line: link gain.

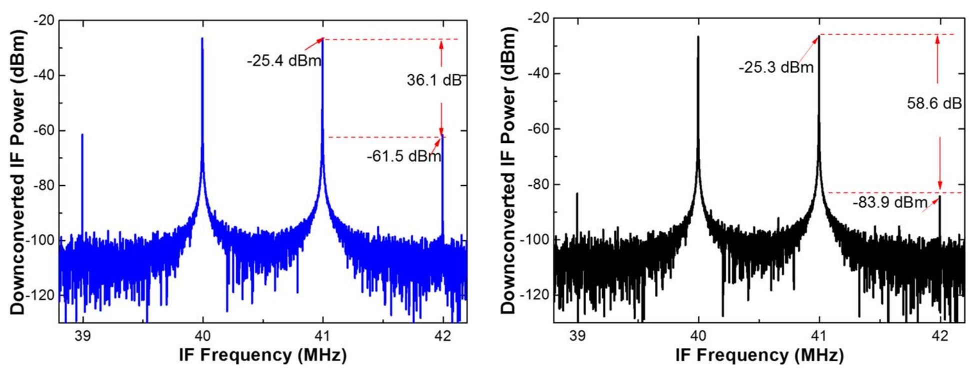

Fig. 4. Received IF spectra (a) before and (b) after the proposed digital linearization.

worthwhile to note that the link gain may be further increased by further decreasing the bias angle (but optical input power higher than 16 dBm is required for maintaining the same I_{PD}). That is, of course, if the detected IF signal is absent of gain saturation (or has tolerable gain saturation). It is also worthwhile to note that the extra nonlinear distortion introduced by the low-biased modulator has limited impact on the sub-octave analog photonics link.

A proof-of-concept experiment is carried out, according to Fig. 2. The digital linearization is performed by an offline MATLAB program. The electrical spectrum comparison between links with and without digital linearization is shown in Fig. 4, when the input RF power is 2 dBm per tone. The down-converted fundamental at 40 MHz and 41 MHz as well as the corresponding intermodulation distortions at 39 MHz and 42 MHz are presented for both cases. Considerable IMD3 is observed due to the intrinsic nonlinear in the IMDD link in Fig. 4(a), with a fundamental to IMD3 ratio of 36.1 dB. After digital linearization, the nonlinearity is significantly suppressed by 22.5 dB. A fundamental to distortion ratio of 58.6 dB is achieved in Fig. 4(b).

The input RF power is scanned while both the fundamental and the intermodulation components are monitored, and the measured IF power value as a function of the input RF power is plotted in Fig. 5. The measured noise floor level around 40 MHz is -162 dBm/Hz, which is dominated by the

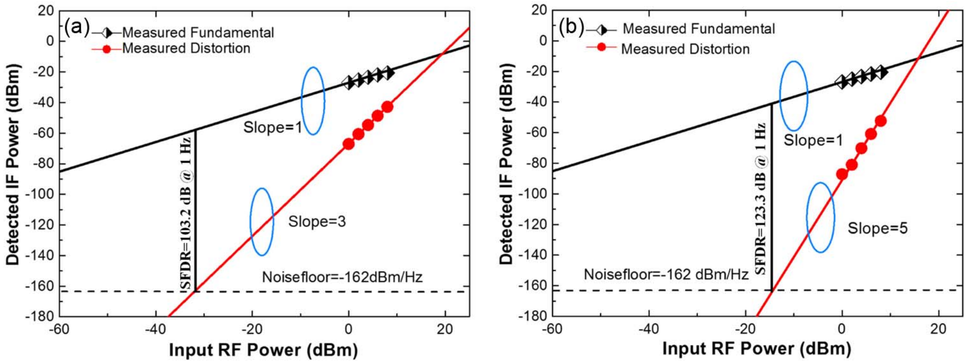

Fig. 5. Measured fundamental and intermodulation components versus the input RF power (a) before and (b) after the proposed digital linearization.

shot noise. By comparing Fig. 5(a) and (b), one can observe a down-conversion SFDR increasing from 103.2 to 123.3 dB @ 1 Hz bandwidth. Compared with a conventional IMDD link, the improvement is as large as 20.1 dB by the proposed digital linearization.

Fig. 5 also shows the well suppression of IMD3. As can be seen in Fig. 5(a), the slope for the measured fundamental component is 1, while it is 3 for the intermodulation component. As a result, the IMD3 dominates the inter-modulation nonlinearity before the digital linearization. In Fig. 5(b), the intermodulation component has a slope of 5 instead, which indicates that the fifth-order intermodulation dominates and IMD3 is completely suppressed by the proposed algorithm. Further suppression of higher-order nonlinearity is under investigation.

4. Conclusion

In conclusion, we proposed and demonstrated a digital linearization technique for the conventional MZM-based intensity-modulation direct-detection analog photonic link. Experimental results showed that the third-order intermodulation distortion was well suppressed. With optical down-conversion, a dynamic range increase from 103.2 to 123.3 dB @ 1 Hz bandwidth was observed. The proposed technique did not complicate the traditional IMDD link. Instead, by low biasing the MZM the key distortion information can be acquired by digital low-pass filtering, so that there is no longer need to rebuild the whole system precisely in the digital domain, and the link gain can be further increased as well. Our theory showed that with the help of hardware acquisition, only the bias angle should be known by the algorithm. The simulation showed an adequate tolerance. It should also worthwhile to note that the proposed algorithm is feasible to circumstances other than MZM, e.g., a link with a RF pre-amplifier.

References

[1] C. Cox, E. Ackerman, G. Betts, and J. Prince, "Limits on the performance of RF-over-fiber links and their impact on device design," *IEEE Trans. Microw. Theory Tech.*, vol. 54, no. 2, pp. 64–66, Feb. 2006.

[2] J. Yao, "Microwave photonics," *J. Lightw. Technol.*, vol. 27, no. 3, pp. 314–335, Feb. 2009.

[3] B. Masella, B. Hraimel, and X. P. Zhang, "Enhanced spurious-free dynamic range using mixed polarization in optical single sideband Mach–Zehnder modulator," *J. Lightw. Technol.*, vol. 27, no. 15, pp. 3034–3041, Aug. 2009.

[4] V. Urick, M. Rogge, P. Knapp, L. Swingen, and F. Bucholtz, "Wide-band predistortion linearization for externally modulated long-haul analog fiber-optic links," *IEEE Trans. Microw. Theory Tech.*, vol. 54, no. 4, pp. 1458–1463, Jun. 2006.

[5] T. Ismail, C. P. Liu, J. E. Mitchell, and A. J. Seeds, "High-dynamic-range wireless-over-fiber link using feedforward linearization," *J. Lightw. Technol.*, vol. 25, no. 11, pp. 3274–3282, Nov. 2007.

[6] A. Karim and J. Devenport, "Low noise figure microwave photonic link," in *Proc. IEEE MTT-S Int. Microw. Symp.*, Jun. 2007, pp. 1519–1522.

[7] A. Karim and J. Devenport, "High dynamic range microwave photonic links for RF signal transport and RF-IF conversion," *J. Lightw. Technol.*, vol. 26, no. 15, pp. 2718–2724, Aug. 2008.

[8] Z. Y. Chen, L. S. Yan, W. Pan, B. Luo, X. H. Zou, Y. H. Guo, H. Y. Jiang, and T. Zhou, "SFDR enhancement in analog photonic links by simultaneous compensation for dispersion and nonlinearity," *Opt. Exp.*, vol. 21, no. 8, pp. 20 999–21 009, Sep. 2013.
[9] P. Li, L. S. Yan, T. Zhou, W. L. Zhang, Z. Y. Chen, W. Pan, and B. Luo, "Improvement of linearity in phase-modulated analog photonic link," *Opt. Lett.*, vol. 38, no. 14, pp. 2391–2393, Jul. 2013.
[10] J. Zhang, A. Nicholas Hone, and T. E. Darcie, "Phase-modulated microwave-photonic link with optical-phase-locked-loop enhanced interferometric phase detection," *J. Lightw. Technol.*, vol. 26, no. 15, pp. 2549–2555, Aug. 2008.
[11] G. Zhu, W. Liu, and H. R. Fetterman, "A broadband linearized coherent analog fiber-optic link employing dual parallel Mach–Zehnder modulators," *IEEE Photon. Technol. Lett.*, vol. 21, no. 21, pp. 1627–1629, Nov. 2009.
[12] C. Lim, A. T. Nirmalathas, K. L. Lee, D. Novak, and R. Waterhouse, "Intermodulation distortion improvement for fiber-radio applications incorporating OSSB+C modulation in an optical integrated-access environment," *J. Lightw. Technol.*, vol. 25, no. 6, pp. 1602–1612, Jun. 2007.
[13] T. R. Clark, S. R. O'Connor, and M. L. Dennis, "A phase-modulation I/Q-demodulation microwave-to-digital photonic link," *IEEE Trans. Microw. Theory Tech.*, vol. 58, no. 11, pp. 3039–3058, Nov. 2010.
[14] T. R. Clark and M. L. Dennis, "Coherent optical phase-modulation link," *IEEE Photon. Technol. Lett.*, vol. 19, no. 16, pp. 1206–1208, Aug. 2007.
[15] Q. Lv, K. Xu, Y. Dai, Y. Li, J. Wu, and J. Lin, "I/Q intensity-demodulation analog photonic link based on polarization modulator," *Opt. Lett.*, vol. 36, no. 23, pp. 4602–4604, Dec. 2011.
[16] P. Li, R. Shi, M. Chen, H. Chen, S. Yang, and S. Xie, "Linearized photonic IF downconversion of analog microwave signals based on balanced detection and digital signal post-processing," in *Proc. Int. Top. Meet. Microw. Photon.*, 2012, pp. 68–71.
[17] R. Duan, K. Xu, J. Dai, Q. Lv, Y. Dai, J. Wu, and J. Lin, "Digital linearization technique for IMD3 suppression in intensity-modulated analog optical links," in *Proc. Int. Top. MWP/APMP*, 2011, pp. 234–237.
[18] A. Fard, S. Gupta, and B. Jalali, "Digital broadband linearization technique and its application to photonic time-stretch analog-to-digital converter," *Opt. Lett.*, vol. 36, no. 7, pp. 1077–1079, Apr. 2011.
[19] D. Lam, A. M. Fard, B. Buckley, and B. Jalali, "Digital broadband linearization of optical links," *Opt. Lett.*, vol. 38, no. 4, pp. 446–448, Feb. 2013.
[20] [Online]. Available: http://www.pharad.com/pdf/bias-controller-brochure.pdf